BMAL1 deletion protects against obesity and non-alcoholic fatty liver disease induced by a high-fat diet

Qiwei Shen (shenqiwei@huashan.org.cn)
Huashan Hospital of Fudan University
Chongwen Zhan
Huashan Hospital of Fudan University
Haoran Chen
Huashan Hospital of Fudan University
Yikai Shao
Huashan Hospital of Fudan University
Bo Xu
Huashan Hospital of Fudan University
Rong Hua
Qiyuan Yao
Huashan Hospital of Fudan University
Wenjuan Liu

Article

Keywords: Non-alcoholic fatty liver disease, Obesity, Circadian rhythm, BMAL1

Posted Date: October 10th, 2023

DOI: https://doi.org/10.21203/rs.3.rs-3380752/v1

Additional Declarations: There is **NO** conflict of interest to disclose

Version of Record: A version of this preprint was published at International Journal of Obesity on December 11th, 2023. See the published version at https://doi.org/10.1038/s41366-023-01435-w.

Abstract

Background and Aims:

Obesity and non-alcoholic fatty liver disease (NAFLD) are major health concerns. The circadian rhythm is an autonomous and intrinsic timekeeping system closely associated with energy metabolism and obesity. Thus, this study explored the role of brain and muscle aryl hydrocarbon receptor nuclear translocator-like1 (BMAL1), a circadian clock regulator, in the development of obesity and NAFLD.

Methods

We generated *BMAL1* knockout (BMAL1 KO) mice to imitate circadian rhythm disruption. The study comprised three groups from the same litter: BMAL1 KO mice fed a high-fat diet (to establish obesity and NAFLD phenotypes), wild-type mice fed normal chow, and wild-type mice fed a high-fat diet. The metabolic and NAFLD phenotypes were assessed via physiological measurements and histological examinations. Quantitative polymerase chain reaction and western blotting were used to identify and validate changes in the signaling pathways responsible for the altered NAFLD phenotypes in the wild-type and BMAL1 KO mice.

Results

BMAL1 depletion protected against obesity and metabolic disorders induced by a high-fat diet. BMAL1 deficiency also relieved hepatic steatosis and decreased cluster of differentiation 36 and peroxisome proliferator-activated receptor gamma (i.e., PPARγ) expression.

Conclusion

BMAL1 plays an important role in the development of obesity and NAFLD and, thus, is a potential therapeutic target for these conditions.

1. Introduction

Over the past 50 years, the prevalence of obesity has increased dramatically, becoming a major global public health issue [1]. Specifically, the global prevalence of obesity tripled between 1975 and 2016, imposing considerable health and economic burdens on society [2]. Complications, such as diabetes, hypertension, non-alcoholic fatty liver disease (NAFLD), and osteoarthritis, accompany obesity [1]. NAFLD is the most common chronic liver disease, affecting approximately 25% of adults worldwide as of 2016. Furthermore, it is a progressive disease that includes non-alcoholic hepatic steatosis with or without mild inflammation, non-alcoholic steatohepatitis, cirrhosis, and hepatocellular carcinoma [3, 4]. The pathogenesis of NAFLD includes metabolic, genetic, and microbial factors but, overall, remains unclear [5].

NAFLD leads to fat pool expansion and ectopic lipid deposition by overnutrition [6]. Macrophage infiltration into visceral adipose tissue creates a pro-inflammatory environment that promotes insulin resistance, leading to increased lipolysis in the adipose tissue and de novo lipogenesis in the liver [7]. Large amounts of lipids form in the liver due to unbalanced lipid metabolism, and ectopic lipid accumulation leads to cellular oxidative stress, inflammasome activation, and apoptosis, promoting liver inflammation, tissue regeneration, and fiber deposition [8].

Lipid metabolism is also regulated by a complex neuroendocrine system, and circadian rhythms are important drivers of NAFLD [9]. The circadian rhythm is an endogenous autonomous timing system that plays an important role in maintaining physiological functions [10]. Circadian disruption contributes to obesity and metabolic diseases, including NAFLD [11]. Consequently, circadian rhythm dysregulation is a key characteristic of NAFLD, regulating the occurrence and progression of NAFLD by affecting nutritional homeostasis, autophagy, glucose metabolism, lipid and bile acid metabolism, endoplasmic reticulum stress, and intestinal microbial metabolism [12, 13].

Circadian rhythms in mammals are controlled by the transcription-translation feedback loop, which comprises various circadian genes, including brain and muscle aryl hydrocarbon receptor nuclear translocator-like1 (*BMAL1*), circadian locomotor output cycles kaput (*CLOCK*), period circadian regulator 1 and 2 (i.e., *PER1* and *PER2*, respectively), cryptochrome circadian regulator 1 (i.e., *CRY1*), RAR-related orphan receptor A (i.e., *RORA*), and *REV-ERB* [14]. BMAL1 and CLOCK heterodimers positively affect the transcription-translation feedback loop and drive the circadian cycle [14] BMAL1 is also closely associated with high-fat diet (HFD)-induced obesity and metabolic disorders [15, 16]. However, the effects of BMAL1 on obesity are controversial, and how BMAL1 affects HFD-induced obesity and metabolic disorders remains unknown [17–19].

Therefore, this study explored the role of BMAL1 in the pathogenesis of obesity and NAFLD to provide new ideas and measures for treating obesity and metabolic diseases, especially NAFLD.

2. Materials and methods

2.1. Animals

Wild-type (WT) and BMAL1 knockout (KO) mice were purchased from the Institute of Model Zoology, Nanjing University, and bred in-house at the Shanghai Model Organisms Center to obtain homozygous and littermate WT mice. The BMAL1 KO mice were fed a 60% HFD (Research Diets D12492, New Brunswick, New Jersey, USA) (BMAL1 KO + HFD, n = 6), and the WT mice (control groups) were fed normal chow (WT + NC, n = 5) or an HFD (WT + HFD, n = 5) for 20 weeks.

All animal experiments were strictly conducted following the National Research Council Guide for the Care and Use of Laboratory Animals and approved by the Department of Laboratory Animal Science, Fudan University.

2.2. Human liver tissues

Liver tissues (approximately 1.5 × 2.0 × 2.0 cm^3) were obtained from patients with obesity during bariatric surgery. The tissues were snap-frozen in liquid nitrogen and stored at − 80 ℃. The Ethics Committee of Huashan Hospital, Fudan University, Shanghai, China, reviewed and approved the study protocols (KY2017-222). All individuals provided written informed consent.

2.3. Intraperitoneal glucose and insulin tolerance test

After 20 weeks, all mice underwent an intraperitoneal glucose tolerance test (IPGTT). The mice were fasted for 12 h before a 10 mg/kg intraperitoneal glucose injection. Blood samples were collected from the tail vein after 0, 15, 30, 60, and 120 min and analyzed using a glucometer (Contour TS, Shanghai, China).

The mice also underwent an intraperitoneal insulin tolerance test (IPITT) after 20 weeks. All the mice were fasted for 4 h before a 0.75 U/kg intraperitoneal insulin injection. Blood samples were collected from the tail vein after 0, 15, 30, 60, and 120 min and analyzed using a glucometer.

2.4. Insulin resistance testing

Blood samples were collected from mice following an overnight fast, and blood glucose levels were measured using a glucometer. The serum insulin levels were also measured using a mouse insulin enzyme-linked immunosorbent assay kit (EMINS, Thermo Fisher Scientific, Waltham, MA, USA). The homeostasis model assessment of insulin resistance (HOMA-IR) was calculated as follows: fasting blood glucose [mmol/L] × fasting serum insulin [mU/L]/22.5.

2.5. Western blot analysis

Liver tissue was lysed with RIPA lysis buffer to extract total protein. The protein concentration was determined using a BCA protein assay kit (Thermo Fisher Scientific). Then, 20 μg of protein were separated on sodium dodecyl-sulfate polyacrylamide gel electrophoresis gels and transferred onto polyvinylidene fluoride membranes (Millipore, Burlington, MA, USA). The membrane was blocked with 5% non-fat milk for 1 h and then incubated with specific primary antibodies overnight at 4 ℃ (anti-BMAL1:1:1000, ab235577; anti-cluster of differentiation 36 [CD36]: 1:1000, ab252922; anti-peroxisome proliferator-activated receptor gamma [PPARγ]: 1:1000, ab272718; anti-glyceraldehyde-3-phosphate dehydrogenase [i.e., GAPDH]: 1:1000, ab8245; and anti-β-ACTIN:1:1000, ab8226; all purchased from Abcam, Cambridge, UK). After incubation, the membrane was washed and incubated with a horseradish peroxidase-conjugated secondary antibody (1:2000, ab288151, purchased from Abcam, Cambridge, UK) for 1 h at room temperature. Protein bands were visualized using enhanced chemiluminescence substrate (Thermo Fisher Scientific). Protein band density was quantified using ImageJ software (National Institute of Health, Bethesda, MD, USA) and normalized to β-actin levels.

2.6. Quantitative real-time polymerase chain reaction

Total RNA was extracted using the TRIzol reagent (Invitrogen/Thermo Fisher Scientific) and reverse-transcribed into complementary DNA using a PrimeScript RT kit (Takara Bio, Beijing, China). Gene expression levels were measured using TB Green Premix (Takara Bio) on a QuantStudio 6 system (Thermo Fisher Scientific). Gene expression levels were normalized to the β-actin level and calculated using the $2^{-\Delta\Delta Ct}$ method to assess the relative changes. Table S1 lists the primer sequences.

2.7. Serum lipid measurements

Blood samples were collected from mice following overnight fasting. Serum total cholesterol (T-CHO), low-density lipoprotein cholesterol (LDL-C), triglycerides (TG), and high-density lipoprotein cholesterol (HDL-C) levels were measured using an automatic biochemical analyzer (Rayto Life and Analytical Sciences, Shenzhen, China).

2.8. Histological examinations

The mouse livers were fixed in 4% paraformaldehyde and embedded in paraffin. All tissues were sliced into 4 μm sections and stained with hematoxylin and eosin (H&E). The NAFLD activity score was measured at 200× high power field (HPF) in three different fields. For fat deposition evaluations, fixed specimens were embedded in optimal cutting temperature compound (Servicebio, Wuhan, China), then serially sliced into 8 μm sections and stained with Oil Red O (ORO). The lipid droplet areas were measured in three different fields under 200× HPF using Image-Pro Plus 6.0 (Media Cybernetics, Rockville, MD, USA).

2.9. Liver TG measurements

Liver tissues were weighed, and lipids were extracted using absolute ethyl alcohol. The TG content was measured using a Triglyceride Assay Kit (A110-1-1, Jiancheng, Nanjing, China) following the manufacturer's instructions.

2.10. Statistical analyses

All data were presented as means ± standard errors of the mean. SPSS (version 26, IBM Corp., Armonk, NY, USA) and GraphPad Prism 9 (GraphPad Inc., San Diego, CA, USA) and software were used for the statistical analyses and plotting, respectively. Comparisons between two groups were performed using Student's t-tests. Comparisons between three or four groups were performed using one-way or two-way analysis of variance tests. *P*-values of < 0.05 were considered statistically significant.

3. Results

3.1. *BMAL1* deficiency prevents HFD-induced obesity and glucose metabolic disorders

Initially (week zero), BMAL1 protein was normally expressed in the livers of WT mice but was undetectable in the BMAL1 KO mice (Fig. 1A). From weeks zero to four, the body weights of WT + NC and

WT + HFD groups increased time-dependently (Fig. 1B, C). However, the weight in the WT + NC group increased slowly and was stable after 20 weeks (32.04 ± 0.56 g). In contrast, the weight in the WT + HFD group continued increasing until the end of the experiment at 20 weeks (49.30 ± 3.57 g).

The baseline weight was lower in the BMAL1 KO + HFD group than in either WT group but increased during the first three weeks of the HFD, becoming similar to that of the WT + HFD group. However, the weight of the BMAL1 KO + HFD group stabilized and became significantly lower than that of the WT + HFD mice starting in week six (Fig. 1B, C).

The IPITT (Fig. 1D, E) and IPGTT (Fig. 1F, G) tests demonstrated that the blood glucose level and the area under the glucose concentration-time curve were higher in the WT + HFD group than in the WT + NC group. However, the values were lower in the BMAL1 KO + HFD group than in the WT + HFD group. Moreover, the fasting blood glucose and insulin levels and HOMA-IR values were lower in the BMAL1 KO + HFD group than in the WT + HFD group (Fig. 1H–J).

3.2. *BMAL1* deficiency prevents HFD-induced lipid metabolism disorders

After 20 weeks, the serum T-CHO, LDL-C, and TG levels were higher in the WT + HFD group than in the WT + NC group. Furthermore, T-CHO and LDL-C levels were lower in the BMAL1 KO + HFD group than in the WT + HFD group; TG levels did not differ among the groups (Fig. 2A–C). The HDL-C level also did not differ among the three groups (Fig. 2D).

The inguinal and epididymal fat weights were significantly higher in the WT + HFD group than in the WT + NC and BMAL1 KO + HFD groups (Fig. 2E, F). H&E staining showed that the areas and amounts of lipid droplets in the inguinal and epididymal fat adipocytes were larger in the WT + HFD group than in the WT + NC and the BMAL1 KO + HFD groups (Fig. 2G, H).

3.3. *BMAL1* deficiency prevents HFD-induced hepatic steatosis

The liver weights and TG levels were significantly higher in the WT + HFD group than in the WT + NC and BMAL1 KO + HFD groups (Fig. 3A, B). Liver histological staining indicated that the WT + HFD group had more fat vacuoles and lipid accumulation than the other groups, indicating severe hepatic steatosis. Specifically, the BMAL1 KO + HFD group had fewer fat vacuoles and less lipid accumulation than the WT + HFD group (Fig. 3C, E). Finally, the liver NAFLD activity scores and ORO-positive areas were significantly higher in the WT + HFD group than in the WT + NC and BMAL1 KO + HFD groups (Fig. 3D, F).

3.4. *BMAL1* deficiency prevents hepatic fatty acid uptake

Genes in the hepatic lipid metabolism pathways were examined to explore the role and potential mechanisms of BMAL1 in hepatic lipid metabolism, including genes related to de novo lipogenesis (acetyl-CoA carboxylase 1 [i.e., *ACC1*] and fatty acid synthase [*FASN*]), fatty acid β-oxidation (peroxisome

proliferator-activated receptor-α [i.e., *PPARα*], carnitine palmitoyltransferase I [i.e., *CPT-1α*], and alternative oxidase [i.e., *AOX*]), and fatty acid uptake (*CD36* and fatty acid binding protein 1 [i.e., *FABP1*]).

FASN expression (de novo lipogenesis) was higher in the WT + HFD group than in the WT + NC and BMAL1 KO + HFD groups. *CD36* expression (fatty acid uptake) had similar results. However, expression of the fatty acid β-oxidation genes did not differ among the groups (Fig. 4A). Furthermore, CD36 protein expression was significantly lower in the BMAL1 KO + HFD group than in the WT + HFD group (Fig. 4B).

Orphan nuclear receptors commonly target CD36, including liver X receptor (LXR), PPARγ, and pregnane X receptor (PXR). Therefore, we explored how BMAL1 regulates CD36 expression by measuring the gene expression of orphan nuclear receptors. *PPARγ* expression was significantly higher in the WT + HFD group than in the WT + NC and BMAL1 KO + HFD groups (Fig. 4C). PPARγ protein expression was also significantly higher in the WT + HFD group than in the BMAL1 KO + HFD group (Fig. 4D). *LXR* and *PXR* expression did not differ among the groups (Fig. 4C).

Finally, we measured *BMAL1* and *PPARγ* gene expression in patients with obesity (n = 32); Table 1 presents their basic characteristics. We identified a significant positive correlation between *BMAL1* and *PPARγ* expression (r = 0.5188, $P = 0.0024$; Fig. 4E).

Table 1
Characteristics of the patients with obesity

Characteristic	Value
Sex (Male/Female) (n)	7/25
Age (years)	28.60 ± 6.00
Body mass index (kg/m^2)	39.10 ± 7.85
Fasting blood glucose (mmol/L)	6.14 ± 1.82
Serum triglyceride (mmol/L)	1.86 ± 1.44
Serum high-density lipoprotein cholesterol (mmol/L)	1.07 ± 0.23
Serum total cholesterol (mmol/L)	4.90 ± 0.73
Serum non-esterified fatty acid (mmol/L)	0.59 ± 0.19

Data are presented as means ± standard errors of the mean unless otherwise stated.

4. Discussion

As an endogenous autonomous timing system, circadian rhythm plays an important role in maintaining the basic physiological functions of the human body. Previous epidemiological studies have confirmed that circadian rhythm disturbances are closely related to the occurrence of obesity and metabolic diseases. However, the molecular mechanisms involved remain unclear [20, 21]. BMAL1 is an important

component of the molecular clock, and previous studies suggest a close relationship between it and the occurrence of obesity and metabolic diseases. In this study, we simulated circadian rhythm perturbations by deleting *BMAL1* in mice to explore its regulatory effects on the development of obesity and metabolic disorders [22].

Decreased BMAL1 expression in obese patients and mice has been previously reported, but its correlation with obesity remains unclear [19]. We found that the BMAL1 KO mice weighed less and had improved metabolic markers than the WT mice fed an HFD. This result suggests that *BMAL1* depletion protects against HFD-induced obesity and metabolic disorders. Thus, BMAL1 may negatively regulate metabolism and play an indispensable role in HFD-induced obesity and metabolic diseases. Previously, it was hypothesized that the loss of BMAL1 would disturb the circadian rhythm, causing obesity and metabolic diseases [15, 23]; our results contradict these perceptions. However, previous studies have shown that *BMAL1* deficiency has a positive regulatory effect on the body, such as improving defenses against bacterial infection and attenuating the development of atherosclerosis [24, 25], consistent with our study's results.

BMAL1 KO mice have been used to explore the role of BMAL1 in obesity and metabolic diseases, but the results remain controversial owing to the various research schedules used in these studies. For instance, Shimba et al. found that *BMAL1* KO induced dyslipidemia and ectopic fat formation in mice fed an HFD for five weeks [17]. However, this result contradicts those of our study, perhaps owing to differences in the duration of the HFD. Furthermore, Jouffe et al. reported that *BMAL1* KO protected against HFD-induced obesity, insulin resistance, and hepatic steatosis in mice fed an HFD for 12 weeks [18]. This result is consistent with ours, suggesting that *BMAL1* KO prevents obesity and metabolic disorders for those on long-term HFDs. Nonetheless, the potential mechanisms by which BMAL1 regulates metabolism remain unclear.

After identifying the effects of *BMAL1* deficiency on obesity and metabolic phenotypes, we aimed to elucidate the underlying molecular mechanisms. As the central organ of energy metabolism, the liver is involved in various metabolic processes, including gluconeogenesis, glycolysis, de novo lipogenesis, fatty acid uptake and oxidation, fat redistribution, and fatty acid transport [26]. Thus, we investigated the effects of *BMAL1* deficiency on lipid deposition and metabolism in the liver to explore the underlying mechanisms. We found that *BMAL1* KO inhibited *CD36* expression, a liver fatty acid uptake gene. CD36 is a transmembrane glycoprotein with a molecular weight of 88 kDa that binds to various ligands and participates in several activities, such as fatty acid uptake, angiogenesis, thrombosis, inflammation, and atherosclerosis [27]. Under normal physiological conditions, CD36 expression in liver cells is very low [27]. However, it significantly increases when metabolic disorders occur, such as obesity and insulin resistance, which promotes liver fatty acid intake, increases liver TG synthesis, and accelerates NAFLD [27]. Our study demonstrated that *BMAL1* deficiency inhibited the HFD-induced increase in CD36 expression in the liver.

Moreover, CD36 is a common target of orphan nuclear receptors, including PPARγ, LXR, and PXR [28, 29]. PPARγ directly up-regulates CD36 expression, while LXR and PXR directly and indirectly (via PPARγ activation) up-regulate CD36 expression [28]. Therefore, we assessed PPARγ, LXR, and PXR expression levels in mouse liver tissues, finding that *BMAL1* deficiency inhibited PPARγ expression. We also evaluated the correlation between *BMAL1* and P*PARγ* gene expression in the liver tissues of patients with obesity, and the results were consistent with those of the animal experiment. In conclusion, we hypothesize that *BMAL1* depletion inhibits hepatic fatty acid uptake and lipid deposition by inhibiting the hepatic PPARγ-CD36 pathway.

Although this study clarifies the regulatory effect of *BMAL1* deficiency on obesity, there are still limitations. We found that *BMAL1* deletion minimized the HFD-induced increase in serum T-CHO and liver TG levels, but serum TG levels did not differ among the groups. Serum TG and T-CHO levels correlate with lipid absorption and synthesis in the intestinal tract, liver, and adipose tissue [30–32]. Our study only examined lipid metabolism in the liver; the intestine and adipose tissue phenotypes remain unknown. Therefore, we plan to conduct subsequent studies on the intestinal tract and adipose tissue to clarify the changes and mechanisms of lipid metabolism in the body more extensively. Moreover, we only studied the effect of *BMAL1* deficiency on PPARγ expression, and it is unclear whether PPARγ participates in BMAL1-mediated CD36 expression and hepatic steatosis. Thus, the specific underlying regulatory effects and mechanisms between BMAL1 and PPARγ require further study.

5. Conclusion

BMAL1 deficiency protects against HFD-induced obesity and hepatic steatosis, perhaps via the PPARγ-CD36 pathway. This study further clarified the role of BMAL1 in obesity and suggests it could be a target for treating obesity and NAFLD in the future.

Abbreviations

NAFLD, non-alcoholic fatty liver disease; BMAL1, brain and muscle aryl hydrocarbon receptor nuclear translocator-like1; CLOCK, circadian locomotor output cycles kaput; PER, period circadian regulator; CRY1, cryptochrome circadian regulator 1; RORA: RAR-related orphan receptor A; HFD, high-fat diet; WT, wild-type; KO, knockout; IPGTT, intraperitoneal glucose tolerance test; IPITT, intraperitoneal insulin tolerance test; HOMA-IR, homeostasis model assessment of insulin resistance; CD36, cluster of differentiation 36; PPARγ, peroxisome proliferator-activated receptor gamma; GAPDH, glyceraldehyde-3-phosphate dehydrogenase; T-CHO, total cholesterol; LDL-C, low-density lipoprotein cholesterol; TG, triglycerides; HDL-C, high-density lipoprotein cholesterol; H&E, hematoxylin and eosin; HPF, high power field; ORO, Oil Red O; ACC1, acetyl-CoA carboxylase 1; FASN, fatty acid synthase; PPARα, peroxisome proliferator-activated receptor-α; CPT-1α, carnitine palmitoyltransferase Iα; AOX, alternative oxidase; FABP1, fatty acid binding protein 1; LXR, liver X receptor; PXR, pregnane X receptor;

Declarations

AUTHOR CONTRIBUTIONS

Wenjuan Liu and Qiwei Shen conceived, designed, and supervised the study. Chongwen Zhan, Haoran Chen, Bo Xu, Yikai Shao, Qiyuan Yao and Rong Hua conducted the study and analyzed the results. Chongwen Zhan wrote the manuscript.

ACKNOWLEDGEMENTS

This study was supported by the National Natural Science Foundation of China (grant numbers 81800751, 81970458, and 82100882). All authors were involved in the decision to submit the article for publication.

CONFLICT OF INTEREST STATEMENT

The authors declare that no conflicts of interest exist.

DATA AVAILABILITY STATEMENT

Data will be made available on request.

References

1. Blüher, M., 2019. Obesity: global epidemiology and pathogenesis. Nat Rev Endocrinol 15:288-298.
2. Abarca-Gómez, L., Abdeen, Z.A., Hamid, Z.A., Abu-Rmeileh, N.M., Acosta-Cazares, B., Acuin, C, et al., 2017. Worldwide trends in body-mass index, underweight, overweight, and obesity from 1975 to 2016: a pooled analysis of 2416 population-based measurement studies in 128.9 million children, adolescents, and adults. Lancet 390:2627-2642.
3. Younossi, Z.M., 2019. Non-alcoholic fatty liver disease - A global public health perspective. J Hepatol 70:531-544.
4. Paik, J.M, Golabi, P., Younossi, Y., Mishra, A., Younossi, Za. M., 2020. Changes in the global burden of chronic liver diseases from 2012 to 2017: The growing impact of NAFLD. Hepatology 72:1605-1616.
5. Pafili, K., Roden, M., 2021. Nonalcoholic fatty liver disease (NAFLD) from pathogenesis to treatment concepts in humans. Mol Metab 50:101122.
6. Younossi, Z.M., Koenig, A.B., Abdelatif, D., Fazel, Y., Henry, L., Wymer, M., 2016. Global epidemiology of nonalcoholic fatty liver disease-Meta-analytic assessment of prevalence, incidence, and outcomes. Hepatology 64:73-84.

7. Friedman, S.L., Neuschwander-Tetri, B.A., Rinella, M., Sanyal, A.J., 2018. Mechanisms of NAFLD development and therapeutic strategies. Nat Med 24:908-922.
8. Sanyal, A.J., 2019. Past, present and future perspectives in nonalcoholic fatty liver disease. Nat Rev Gastroenterol Hepatol 16:377-386.
9. Gnocchi, D., Custodero, C., Sabbà, C., Mazzocca, A., 2019. Circadian rhythms: a possible new player in non-alcoholic fatty liver disease pathophysiology. J Mol Med (Berl) 97:741-759.
10. Pilorz, V., Helfrich-Förster, C., Oster, H., 2018. The role of the circadian clock system in physiology. Pflugers Arch 470:227-239.
11. Bass, J., Lazar, M.A., 2016. Circadian time signatures of fitness and disease. Science 354:994-999.
12. Saran, A.R., Dave, S., 2020. Zarrinpar A. Circadian rhythms in the pathogenesis and treatment of fatty liver disease. Gastroenterology 158:1948-1966.e1.
13. Shetty, A., Hsu, J.W., Manka, P.P., Syn, W.K., 2018. Role of the circadian clock in the metabolic syndrome and nonalcoholic fatty liver disease. Dig Dis Sci 63:3187-3206.
14. Patke, A., Young, M.W., Axelrod, S., 2020. Molecular mechanisms and physiological importance of circadian rhythms. Nat Rev Mol Cell Biol 21:67-84.
15. Marcheva, B., Ramsey, K.M., Buhr E.D., Kobayashi, Y., Su, H., Ko, C.H., et al., 2010. Disruption of the clock components CLOCK and BMAL1 leads to hypoinsulinaemia and diabetes. Nature 466:627-631.
16. Birky, T.L, Bray, M.S., 2014. Understanding circadian gene function: animal models of tissue-specific circadian disruption. IUBMB Life 66:34-41.
17. Shimba S., Ogawa T., Hitosugi S, Ichihashi, Y., Nakadaira, Y., Kobayashi, M., et al., 2011. Deficient of a clock gene, brain and muscle Arnt-like protein-1 (BMAL1), induces dyslipidemia and ectopic fat formation. PLoS One 6:e25231.
18. Jouffe, C., Weger, B.D., Martin, E., Atger, F., Weger, M., Gobet, C., et al., 2022. Disruption of the circadian clock component BMAL1 elicits an endocrine adaption impacting on insulin sensitivity and liver disease. Proc Natl Acad Sci USA 119:e2200083119.
19. Shen Q., Yang Y., Liu W., Wang M., Shao Y., Xu B., et al., 2017. Organ-specific alterations in circadian genes by vertical sleeve gastrectomy in an obese diabetic mouse model. Sci Bull (Beijing) 62(7):467-469.
20. Lim, Y.C., Hoe, V.C.W., Darus, A., Bhoo-Pathy, N., 2018. Association between night-shift work, sleep quality and metabolic syndrome. Occup Environ Med 75:716-723.
21. Gan, Y., Yang, C., Tong, X., Sun, H., Cong, Y., Yin, X., et al., 2015. Shift work and diabetes mellitus: a meta-analysis of observational studies. Occup Environ Med 72:72-78.
22. Kondratov, R.V., Kondratova, A.A., Gorbacheva, V.Y., Vykhovanets, O.V., Antoch, M.P., 2006. Early aging and age-related pathologies in mice deficient in BMAL1, the core componentof the circadian clock. Genes Dev 20:1868-1873.
23. Shi, S.Q., Ansari, T.S., Mcguinness, O.P., Wasserman, D.H., Johnson, C.H., 2013. Circadian disruption leads to insulin resistance and obesity. Curr Biol 23:372-381.

24. Yang, G., Zhang, J., Jiang, T., Monslow, J., Tang, S. Y., Todd, L., et al., 2020. Bmal1 deletion in myeloid cells attenuates atherosclerotic lesion development and restrains abdominal aortic aneurysm formation in hyperlipidemic mice. Arterioscler Thromb Vasc Biol 40:1523-1532.
25. Kitchen, G.B., Cunningham, P.S., Poolman, T.M., Iqbal, M., Maidstone, R., Baxter, M., et al., 2020. The clock gene Bmal1 inhibits macrophage motility, phagocytosis, and impairs defense against pneumonia. Proc Natl Acad Sci USA 117:1543-1551.
26. Rui, L., 2014. Energy metabolism in the liver. Compr Physiol 4:177-197.
27. Rada, P., González-Rodríguez, Á., García-Monzón, C., Valverde, Á.M., 2020. Understanding lipotoxicity in NAFLD pathogenesis: is CD36 a key driver? Cell Death Dis 11:802.
28. Zhou, J., Febbraio, M., Wada, T., Zhai, Y., Kuruba, R., He, J., et al., 2008. Hepatic fatty acid transporter Cd36 is a common target of LXR, PXR, and PPARgamma in promoting steatosis. Gastroenterology 134:556-567.
29. Xiao, Y., Kim, M., Lazar, M.A., 2021. Nuclear receptors and transcriptional regulation in non-alcoholic fatty liver disease.Mol Metab 50:101119.
30. Ko, C.W., Qu, J., Black, D.D., Tso, P., 2020. Regulation of intestinal lipid metabolism: current concepts and relevance to disease. Nat Rev Gastroenterol Hepatol 17:169-183.
31. Jones, J.G., 2016. Hepatic glucose and lipid metabolism. Diabetologia 59:1098-103.
32. Grabner, G.F., Xie, H., Schweiger, M., Zechner, R., 2021. Lipolysis: cellular mechanisms for lipid mobilization from fat stores. Nat Metab 3:1445-1465.

Figures

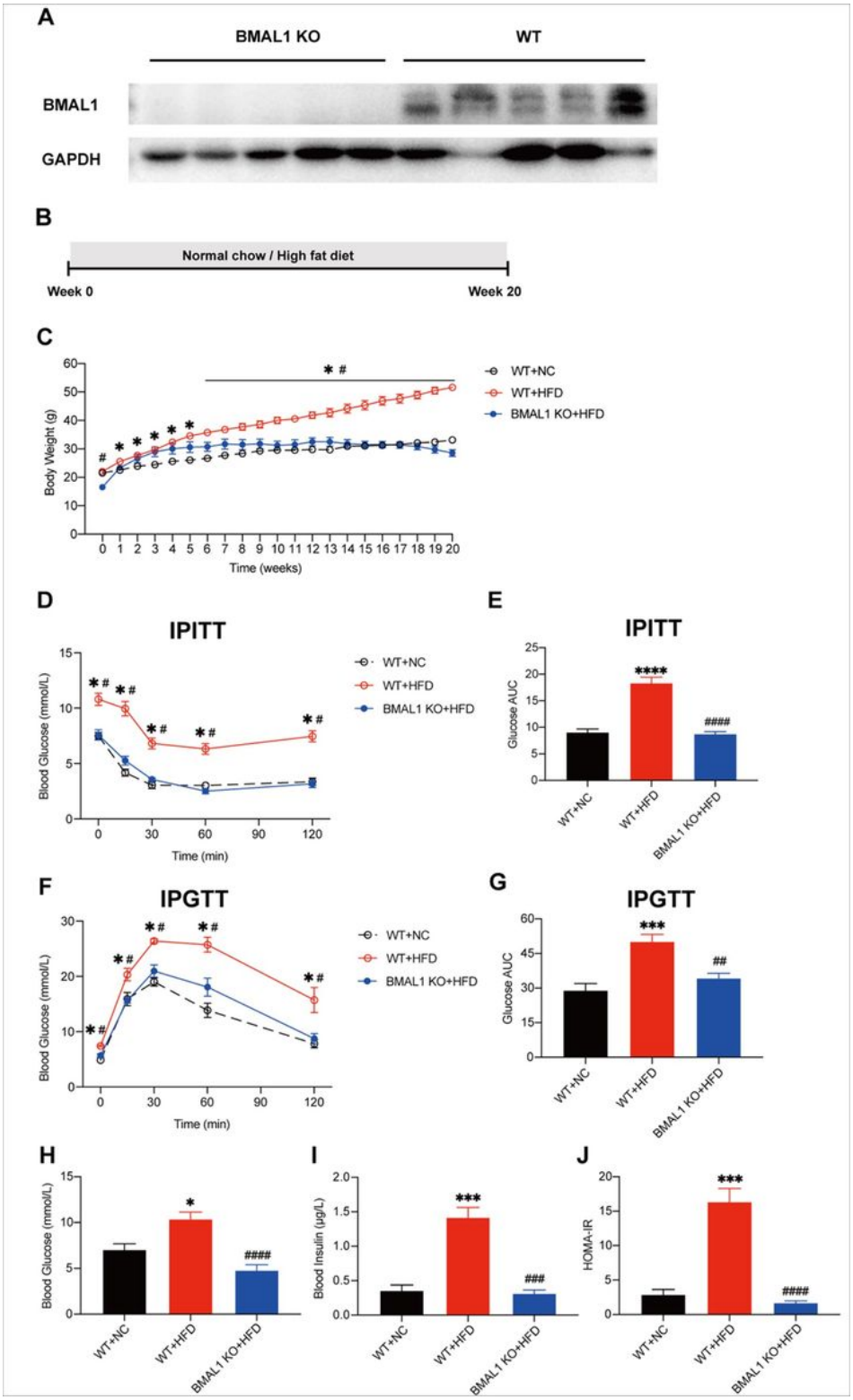

Figure 1

Body weights and glucose metabolism biomarker levels in wild type (WT) and brain and muscle aryl hydrocarbon receptor nuclear translocator-like1 (*BMAL1*) global knockout (BMAL1 KO) mice after 20 weeks of normal chow (NC) or a high-fat diet (HFD). (A)Initial BMAL1 protein levels in the liver of WT and BMAL1 KO mice. (B) The 20-week feeding schedule of the WT and BMAL1 KO mice. (C) Body weight changes over time. (D)Intraperitoneal insulin tolerance test (IPITT) results. (E) Area under the IPITT curve.

(F) Intraperitoneal glucose tolerance test (IPGTT) results. (G) Area under the IPGTT curve. (H) Fasting blood glucose levels. (I)Fasting blood insulin levels. (J) Homeostasis model assessment of insulin resistance (HOMA-IR). *, # $P<0.05$; ## $P<0.01$; ***, ### $P<0.001$; ****, #### $P<0.0001$. *, ***, **** WT+NC vs. WT+HFD; #, ##, ###, #### WT+HFD vs. BMAL1 KO+HFD. Data are presented as means ± standard errors of the mean.

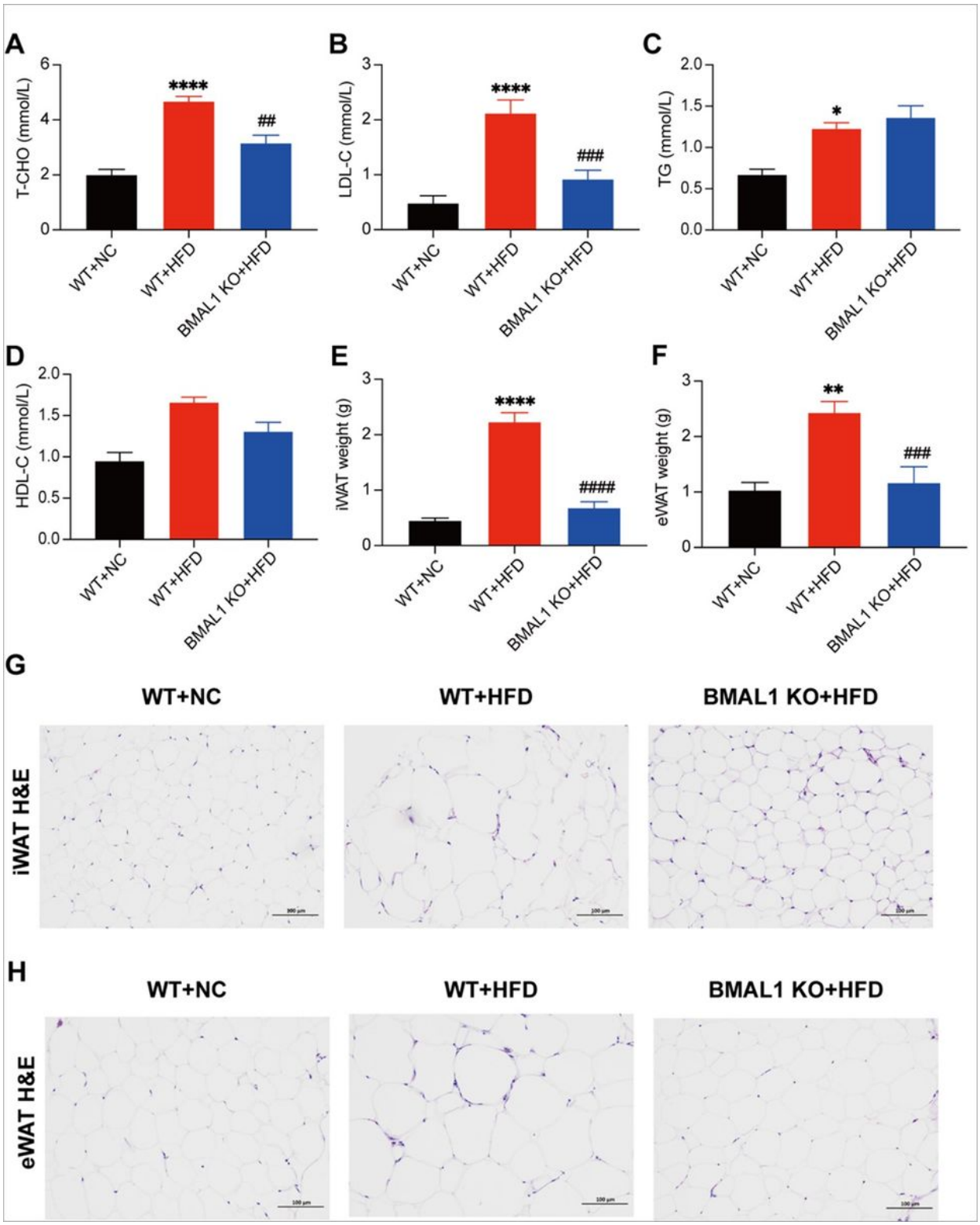

Figure 2

Lipid metabolism phenotypes in wild-type (WT) and brain and muscle aryl hydrocarbon receptor nuclear translocator-like1 (*BMAL1*) global knockout (BMAL1 KO) mice fed normal chow (NC) or a high-fat diet (HFD). (A) Serum total cholesterol (T-CHO) levels. (B) Serum low-density lipoprotein cholesterol (LDL-C) levels. (C) Serum triglyceride (TG) levels. (D) Serum high-density lipoprotein cholesterol (HDL-C) levels. (E) Inguinal fat (iWAT) weight. (F) Epididymal fat (eWAT) weight. (G) Hematoxylin and eosin (H&E) staining of iWAT (200×; scale bar, 100 μm). (H) H&E staining of eWAT (200×; scale bar, 100 μm). * P<0.05; **, ## P<0.01; ### P<0.001; ****, #### P<0.0001. *, **, **** WT+NC vs. WT+HFD; ##, ###, #### WT+HFD vs. BMAL1 KO+HFD. Data are presented as means ± standard errors of the mean.

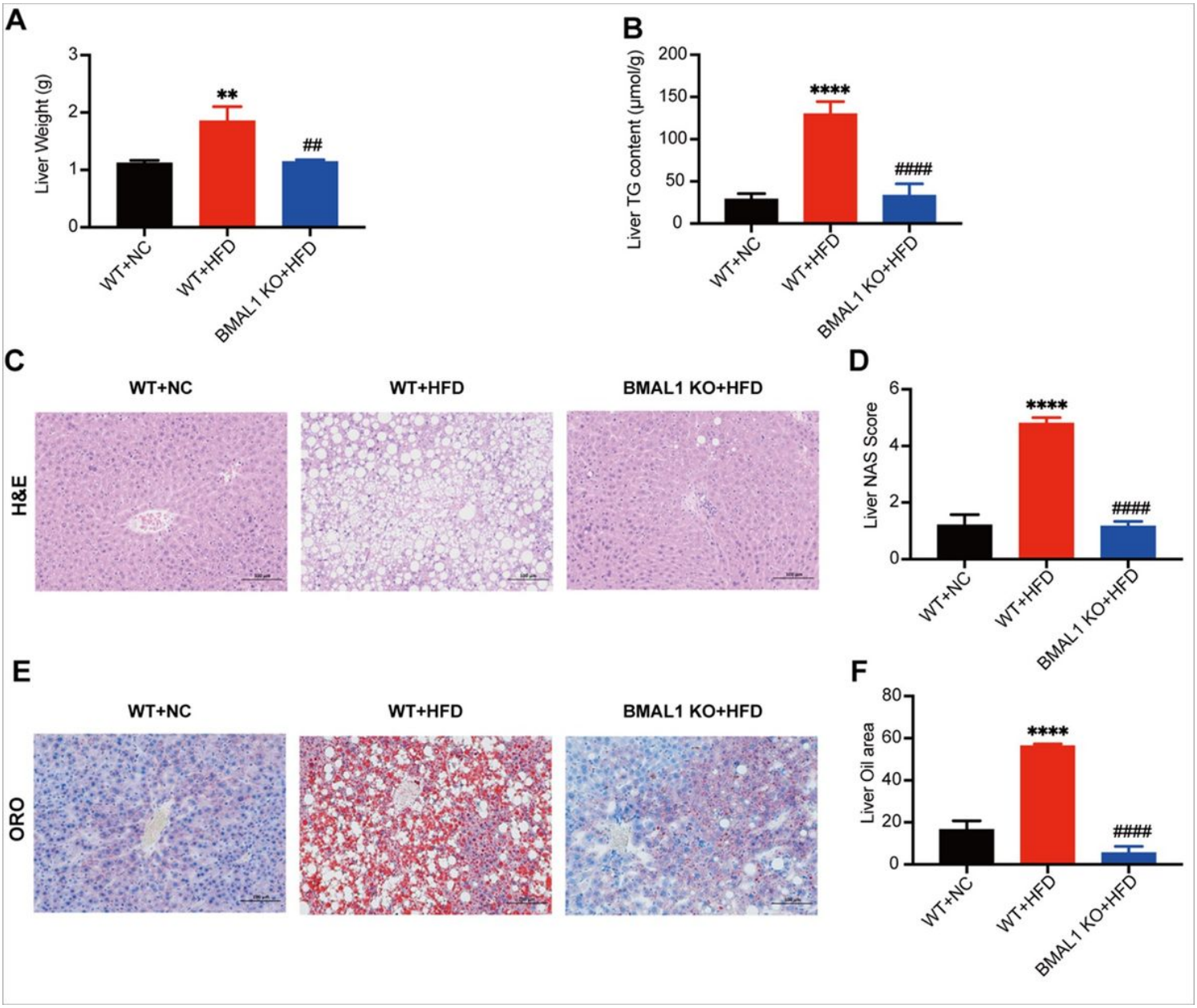

Figure 3

Hepatic lipid metabolism phenotype in wild-type (WT) and brain and muscle aryl hydrocarbon receptor nuclear translocator-like1 (*BMAL1*) global knockout (BMAL1 KO) mice fed normal chow (NC) or a high-fat

diet (HFD). (A) Liver weights. (B)Liver triglyceride (TG) levels. (C) Hematoxylin and eosin (H&E) staining of the liver (200×; scale bar, 100 μm). (D) Liver non-alcoholic fatty liver disease activity scores (NAS). (E) Oil Red O (ORO) staining of the liver (200×; scale bar, 100 μm). (F) ORO-positive areas of the liver. **, ## P <0.01; ****, #### P<0.0001; **, **** WT+NC vs. WT+HFD. ##, #### WT+HFD vs. BMAL1 KO+HFD. Data are presented as means ± standard errors of the mean.

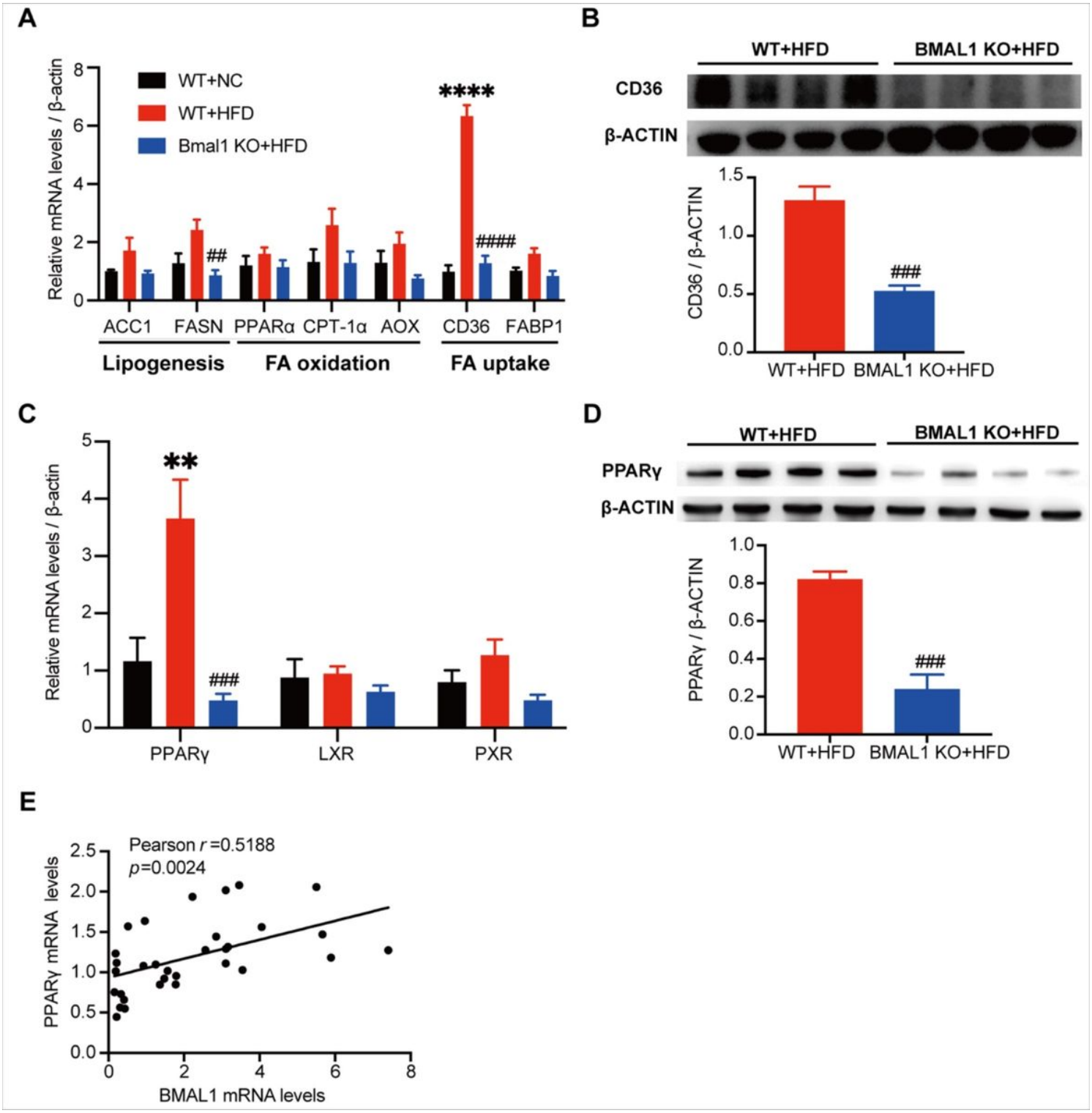

Figure 4

Liver lipid metabolism-related and nuclear receptor gene expression levels in wild-type (WT) and brain and muscle aryl hydrocarbon receptor nuclear translocator-like1 (*BMAL1*) global knockout (BMAL1 KO) mice fed normal chow (NC) or a high-fat diet (HFD). (A) Lipid metabolism-related genes, including those related to lipogenesis (acetyl-CoA carboxylase [*ACC1*] and fatty acid synthase [*FASN*]), fatty acid β-oxidation (peroxisome proliferator-activated receptor-α [*PPARα*], carnitine palmitoyltransferase 1-alpha [*CPT-1α*], and alternative oxidase [*AOX*]), and fatty acid uptake (cluster of differentiation 36 [*CD36*] and fatty acid binding protein 1 [*FABP1*]). (B) CD36 protein levels. (C) Gene expression levels of orphan nuclear receptors. (D)PPARγ protein levels. (E)Correlation between liver *PPARγ* and *BMAL1* gene expression in patients with obesity (Pearson's correlation coefficient). mRNA: messenger RNA. **, ## P <0.01; ### P <0.001; ****, #### P <0.0001. **, **** WT+NC vs. WT+HFD; ##, ###, #### WT+HFD vs. BMAL1 KO+HFD. Data are presented as means ± standard errors of the mean.

Supplementary Files

This is a list of supplementary files associated with this preprint. Click to download.

- Supplementarydata.docx